Continuous Measurements of the Water Activities of Aqueous Droplets of Water-Soluble Organic Compounds

Man Yee Choi and Chak K. Chan*

Department of Chemical Engineering, Hong Kong University of Science and Technology, Clear Water Bay, Kowloon, Hong Kong, China

Received: October 17, 2001; In Final Form: January 30, 2002

Water-soluble organic compounds have recently received much attention because of their ability to absorb water and affect the radiation balance and the climate. Partly because of their relatively high volatility, thermodynamic data on water-soluble organic compounds are scarce. Recently, we have developed a method based on the scanning electrodynamic balance (SEDB) that enables the measurement of water activity data of evaporating droplets within an hour, which can potentially be used to measure volatile species. This paper demonstrates the use of the SEDB to study the hygroscopic growth of selected atmospheric species, including semivolatile organic species with vapor pressure up to 1×10^{-4} mmHg. We also measured the water activities, the crystallization relative humidity, and the deliquescence relative humidity (DRH) of aqueous solutions of maleic acid and glutaric acid. The DRHs of maleic acid and glutaric acid are in general agreement with the literature, except that glutaric acid shows a small delay in the completion of deliquescence due to mass-transfer limitation. The water activities of equal molar mixtures of maleic acid and malic acid and of malonic acid and glutaric acid were also measured. The Zdanovskii−Stokes−Robinson (ZSR) predictions agree well with the measurements of the mixtures. The UNIFAC (UNIQUAC functional group activity coefficients) predictions, using the modified functional group interaction parameters of COOH, OH, and H_2O derived from our earlier measurements of the water activities of aqueous droplets of a list of dicarboxylic and multifunctional acids, are also in agreement with the mixture data.

Introduction

Water-soluble atmospheric aerosols, which are hygroscopic by nature, undergo size changes in moist air. These size changes affect the size distribution, deposition characteristics, radiative properties, and chemical reactivity of atmospheric aerosols. All of these properties are crucial in understanding many other relevant atmospheric processes, such as the earth's radiation balance,[1,2] air pollution,[3] fog formation, and cloud physics[4] as well as visibility degradation.[5] To assess accurately the role that aerosols play in these processes, it is important to determine the physical and chemical properties of atmospheric aerosols under varying humidities. Nondeliquescent hygroscopic aerosols absorb water without an apparent threshold as the relative humidity (RH) increases. The size of a deliquescent aerosol remains unchanged until the RH reaches its corresponding deliquescence RH (DRH) value, which corresponds to the saturation point of the particle in water. Above the DRH, the particle completely dissolves and becomes a droplet. Multicomponent aerosols exhibit more complicated solid−solution phase equilibrium behavior.[6−8]

Recently, atmospheric water-soluble organic compounds (WSOC) have received much attention because of their ability to absorb water and hence their potential to affect the global radiation balance and the climate.[9−12] Although there have been recent measurements of the hygroscopic properties of organic salts and carboxylic acids of atmospheric relevance,[13−15] thermodynamic data on WSOC are scarce, in general, partly because of their relatively high volatility. The development of thermodynamic models including organic species is still at its infancy.[16] The UNIFAC (UNIQUAC functional group activity coefficients) model has been proposed for this application by a few researchers.[17,18] However, it does not work very well on low molecular weight dicarboxylic acids because of the proximity of the carboxylic acid groups. By using water activity data of a few dicarboxylic acids measured in an electrodynamic balance, we have recently parametrized the interaction parameters among H_2O and the COOH and OH groups.[15] However, these modified parameters have not been tested on mixtures and other WSOC.

In hygroscopic growth experiments, the growth ratio in terms of the mass or diameter ratio of an aerosol equilibrated at high RH over that at low RH is determined. Most experimental studies of hygroscopic growth involve increasing the RH in discrete steps.[19,20] These step changes are created by standard solutions of known water vapor pressures, by mixing a saturated stream of air with a dry one or by controlling the absolute water vapor pressure in evacuated systems. While this approach can be used to study the trends of hygroscopic growth of nonvolatile species, the long experiment times make it inapplicable to the measurement of the hygroscopic growth of volatile species.[19] Evacuated systems are useful in reducing the time of measurement, but they may not be easily adaptable to studying volatile species.[13,21]

Our group has recently developed a "dynamic" technique that continuously measures the water activity of evaporating aerosols on the basis of a calibrated decrease in the relative humidity of the feed to an electrodynamic balance (EDB).[22] This technique, called scanning EDB (SEDB) hereafter, involves the scanning

* To whom correspondence should be addressed. E-mail: keckchan@ust.hk. Tel: (852) 2358-7124. Fax: (852) 2358-0054.

10.1021/jp013875o CCC: $22.00
Published on Web 04/17/2002

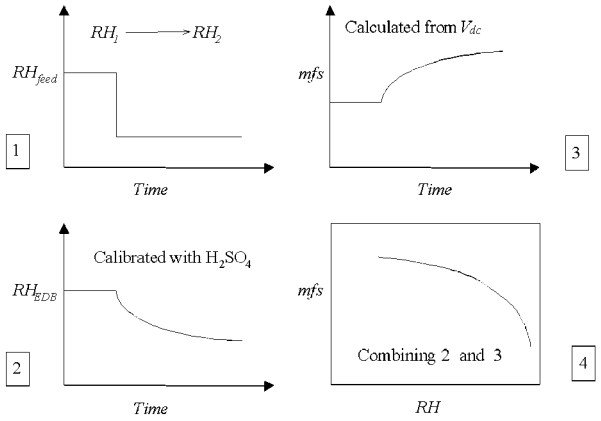

Figure 1. Principle of the scanning electrodynamic balance (SEDB).

of the RH of the EDB, as compared to the stepwise changes of the RH, which are very time-consuming. The SEDB has been demonstrated to be able to provide water activity measurements of evaporating droplets of various inorganic systems within an hour.[22−25] The SEDB is potentially an ideal technique to measure the hygroscopic properties of semivolatile WSOC.

This paper extends the use of the SEDB to studying the hygroscopic growth of aerosols, particularly semivolatile species. Water cycle (growth and evaporation) data of glycerol, malonic acid, maleic acid, and glutaric acid are presented. Malonic, maleic, and glutaric acid have been found in field measurements.[26−28] Glycerol is chosen because it is expected to exist in the atmosphere[29] and can be used as a model WSOC. The water activities of mixtures of maleic acid and malic acid as well as malonic acid and glutaric acid will be reported and compared with the predictions of the Zdanovskii−Stokes−Robinson (ZSR) equation[30,31] and the UNIFAC model.

Methods

The principle of the EDB has been well-documented[32] and therefore is not described here. It suffices to mention that the mass fraction of the solute (mfs = mass of solute on a dry basis/mass of solution) of a levitated particle as a function of ambient RH can be determined. When the EDB operates at ambient pressure with a stream of air of adjustable RH, a set of water activity−aerosol composition measurements can take several hours to a day to accomplish by stepwise changes of the RH.

To explain the principle of the SEDB, it is illustrative to understand how the water activities of evaporating aerosols are measured.[22] Initially, a particle with a diameter of 10−15 μm is equilibrated at high RH (e.g., 80%). Then, the RH in the feed to the EDB is suddenly reduced (step 1 in Figure 1). As a result of this step decrease, the RH at the center of the EDB, where the levitated particle is located, decreases gradually (step 2). By considering the response of a levitated particle to a step decrease in the RH of the feed to the EDB, Liang and Chan[22] confirmed that the rate-limiting step in the evaporation of a droplet levitated in the EDB is the change of the RH inside the EDB. Hence, the particle is always in quasi-equilibrium with its ambient environment. The water content and the mfs of the particle will then change according to the change of RH and its hygroscopic characteristics (step 3). The time dependence of RH, RH(t), is determined by calibration experiments using a species such as H_2SO_4 or other species of which the water activity−concentration dependence is well-known. Finally, when both mfs(t) and RH(t) are known, the mfs(RH) relationship of the species studied can be obtained (step 4). Hence, water activity data can be obtained with a single step change of RH, which reduces the time for measurement to less than an hour. The scanning EDB has been used to measure the water activities of mixtures of sodium, magnesium, and ammonium salts.[23−25]

In experiments to measure particle growth, a step *increase* in the RH of the feed to the EDB is introduced. The experimental setup for growth measurements is identical to that used in earlier evaporation measurements and has been described in detail elsewhere.[22] The experimental procedure is briefly described here. Initially, a particle is equilibrated at the reference state (RH = 80%) for which the balancing voltages with and without air flow (i.e., with and without drag force) are measured. These measurements are needed to calculate the mfs of the particle equilibrated at other RH values. Measurements without air flow at the selected preset RH are referred as "stepwise" measurements in this paper. Then, the feed of the RH is reduced to a low value, RH_1, usually 40%, to begin the hygroscopic growth study. After the particle attains equilibrium at RH_1, a calibrated step change of RH_1 to RH_2 (e.g., 90% RH) is introduced to the EDB to initiate particle growth. The balancing voltage of the growing particle as a function of time, $V(t)$, is measured manually at intervals of roughly 10 s. The mass fraction of the solute (mfs) as a function of RH (= water activity (a_w) × 100 at equilibrium) is obtained by combining $V(t)$ and RH(t). RH(t) is obtained by calibration experiments using NaBr solution droplets at the same experimental conditions. NaBr was chosen because it does not crystallize even at RH = 20% and its water activity data are available.[19] During growth (or evaporation), the change in drag force as a result of the change in particle size due to the change in RH is accounted in the force balance equation of the particle.[22] The overall experimental error in this work is within ±0.01 mfs for droplets, although it can be as large as ±0.02 mfs for partially crystallized or solid particles. All measurements are made at 20−23 °C. In each individual study, the temperature varies less than 0.2 °C. Deviations of water activity within such small temperature changes are not expected to be significant. The error in the determination of RH depends on the flow rate of the feed stream, and it is estimated to be ±0.86% at RH = 40−80%.

In the SEDB measurements, the densities of the particles are required to calculate the mfs. Expressions for the densities of solutions of H_2SO_4, $Ca(NO_3)$, $CaCl_2$, $MgCl_2$, and $MgSO_4$, including supersaturated solutions at 25 °C, are taken from the work of Tang and Munkelwitz,[20] Lobo,[33] Perry,[34] and Tang.[35] The densities of the solutions of organic species are calculated from the mass fraction of the organic species in the droplet and the pure solid density provided by the manufacturer. The densities of the mixtures are estimated from a simple volume additivity rule,[35] which has been found to be adequate for most aqueous multicomponent solutions.

The water activities of bulk solutions were measured using an AquaLab water activity meter (model 3TE, Decagon devices, USA), and the procedures used in measuring the a_w of the bulk solutions are described in detail by Peng and Chan.[14] All bulk measurements are made at 22 °C.

Results and Discussion

1. Hygroscopic Growth of Binary Solutions. To validate the SEDB for studying particle growth, H_2SO_4, $Ca(NO_3)$, $CaCl_2$, $MgCl_2$, and, notably, malonic acid and glycerol were used as test chemicals. The aqueous droplets of these species do not effloresce at RH_1 (40%) and therefore absorb water continuously as the RH increases. Hysteresis in the water cycle of typical

TABLE 1: Experimental Conditions for Each Species Studied

species	RH_1 (%)	RH_2 (%)	range of a_w measured	T (°C)	range of literature a_w	sources of literature data
H_2SO_4	40	90	0.4−0.8	20.1	0.028−0.99	Perry[34]
$CaCl_2$	40	90	0.4−0.8	20.0	0.15−0.99	Cohen et al.[19]
$Ca(NO_3)_2$	40	90	0.4−0.8	20.2	0.14−0.99	Stokes and Robinson[37]
$MgCl_2$	40	90	0.4−0.8	20.1	0.30−0.80	Ha and Chan[23]
$MgSO_4$	40/10	90/70	0.1−0.8	20.0	0.32−0.85	Ha and Chan[23]
malonic acid	40	90	0.4−0.8	23.3	0.10−0.91	Peng et al.[15]
glycerol	80[a]	20[a]	0.2−0.8	22.8	0.39−0.99	Ninni et al.[17]
	20[b]	90[b]				
maleic acid	80	20	0.2−0.8	22.7	N/A[c]	N/A
	20	90				
malic acid	N/A	N/A	N/A	N/A	0.05−0.85	Peng et al.[15]
glutaric acid	80	20	0.2−0.86	23.1	0.04−0.87	Peng et al.[15]
	60	95				
maleic acid + malic acid[d]	80	20	0.2−0.8	22.7	N/A	N/A
	20	90				
malonic acid + glutaric acid[d]	80	20	0.2−0.8	23.0	N/A	N/A
	20	90				

[a] Evaporation study. [b] Growth study. [c] N/A = not available. [d] In 1:1 mole ratio.

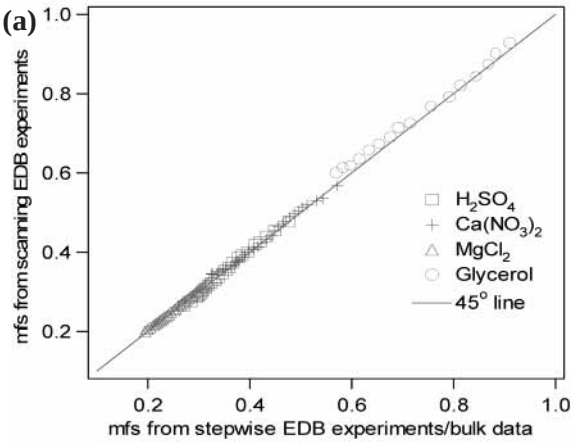

Figure 2. Verification of the SEDB (a) for hygroscopic growth measurement and measured mfs against literature mfs (b) for $MgSO_4$.

deliquescent species was not observed for these chemicals. Table 1 lists the experimental conditions of the growth measurements. The growth of $MgSO_4$, which has been found to exhibit significant mass-transfer limitations during evaporation,[24,36] was also studied.

Figure 2a,b shows that the measured mfs at different RHs are consistent with the data published by Perry[34] for H_2SO_4, by Stokes and Robinson[37] for $Ca(NO_3)_2$, by Ha and Chan[23] for $MgCl_2$ and $MgSO_4$, by Ninni et al.[17] for glycerol, and by Peng et al.[15] for malonic acid. The scanning measurements of $CaCl_2$ are also consistent with published data,[19] although they are not

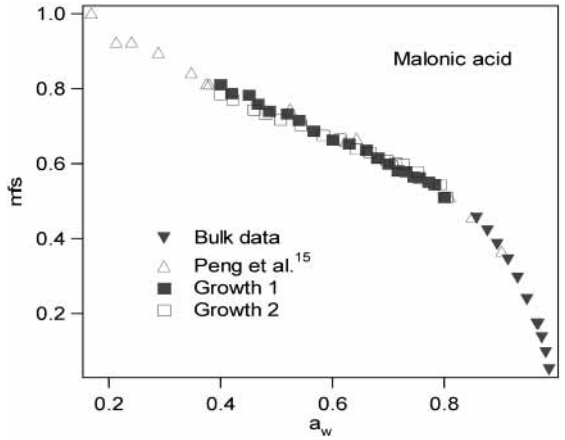

Figure 3. Water activities of malonic acid.

shown in Figure 2a for clarity. All species except for $MgSO_4$ show standard deviations of less than 0.02 in their mfs.

Malonic acid is a semivolatile organic acid. Its water activity−mfs relationship is shown in Figure 3. Peng et al.[15] conducted conventional stepwise EDB measurements of the water activities of malonic acid and found that the evaporation loss was significant. In particular, there was about 3% solute loss per hour at RH = 50% at room temperature and pressure for a droplet of 10−15 μm in diameter. The solute evaporation rate is even higher at low RH. The extent of evaporation was too large to compile a complete data set, which requires about 10 h. To circumvent this problem, Peng et al. recalibrated the droplet at RH = 85% before and after each water activity measurement. Overall, the time to measure a set of water activity data was roughly doubled. However, the solute loss for each data point was controlled to within 2−3%, which is acceptable considering the experimental difficulties and the lack of literature data on this species. As shown in Figure 3, the SEDB measurements are consistent with the stepwise measurements reported by Peng et al.[15]

The SEDB data for glycerol are shown in Figure 4. Glycerol is miscible with water and has a vapor pressure of $(1.06-1.69) \times 10^{-4}$ mmHg (ref 38). Water activity data are available for $a_w > 0.399$ (ref 17). During evaporation, a relatively sharp increase in mfs occurs at RH $\approx$ 29%. This may be due to the formation of a supercooled liquid at a high concentration of glycerol. The crystalline state of glycerol is seldom reached because it has a strong tendency toward supercooling and toward the formation of a solid glassy state.[39] Glycerol absorbs water

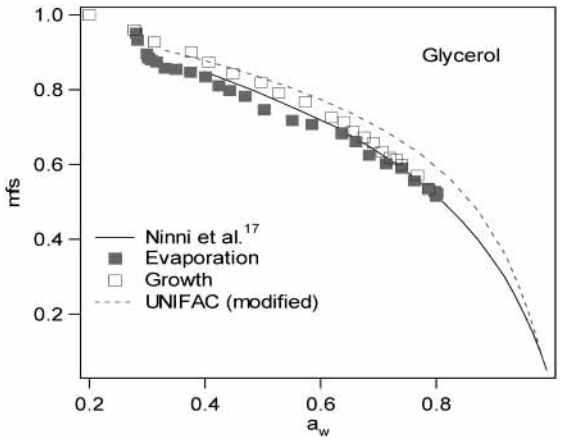

Figure 4. Water activities of glycerol. UNIFAC (modified) represents the prediction by the modified UNIFAC equation.

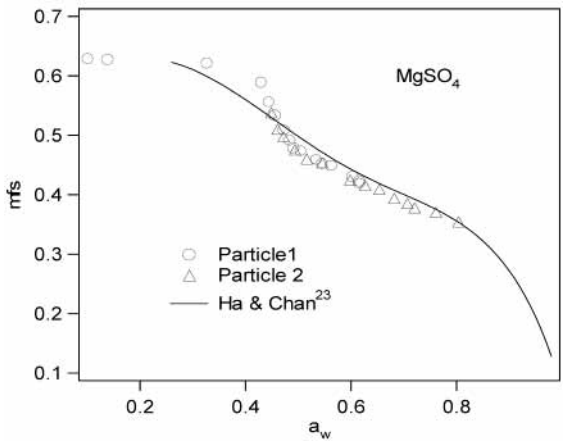

Figure 5. Water activities of evaporating $MgSO_4$ droplets.

following the trend reported in the literature data without any abrupt decrease in mfs, indicating that it does not undergo deliquescence. In general, our data are consistent with the literature with a standard deviation of less than 0.018. The small discrepancy between the growth and evaporation data may be due to the slight mass-transfer effects of concentrated glycerol at low RH. Ray et al.[40] measured the evaporation and growth kinetics of aqueous droplets of glycerol in an EDB and found that the glycerol evaporation rate at a given RH is in general about 1.9 times higher than that of a completely mixed droplet at the corresponding equilibrium composition. They inferred that the interfacial composition of the droplet is not identical to the bulk equilibrium composition because of mass-transfer effects within the particle. The time scale of the unusually slow growth observed in Ray et al.[40] (360 s) is still smaller than the time scale for the RH change in the EDB (440 s). Hence, we did not observe a drastic effect of mass transfer in glycerol droplets. As will be shown later, the growth of $MgSO_4$ droplets shows a much more significant mass-transfer effect.

The UNIFAC (UNIQUAC functional group activity coefficients) model has been found to be useful for predicting thermodynamic properties, including the a_w, of WSOC.[15,38] It involves the description of molecular structures in terms of the constituent-independent functional groups (e.g., CH_2, CH, OH, COOH) and their physical and interaction group parameters. Most of the parameters are available in the literature (e.g., ref 41). Peng et al.[42] demonstrated that the UNIFAC predictions of a_w for glucose, citric acid, and sorbitol are only satisfactory. On the basis of the single-particle water activity measurements of malonic acid, citric acid, malic acid, tartaric acid, oxalic acid, succinic acid, and glutaric acid from dilute solutions to highly supersaturated solutions, Peng et al.[15] modified the interaction parameters of the COOH and OH, COOH and H_2O, and H_2O and OH groups. These modified interaction parameters reduce the deviation between the measurements and the UNIFAC predictions of malic acid from 98% to 38%. Although glycerol is not included in the modified UNIFAC interaction parameters, the modified UNIFAC predictions are satisfactorily consistent with the measurements as shown in Figure 4. The deviation between the predictions and the measurements can be explained from the strong interactions between the three adjacent OH groups on the glycerol molecule, which is one of the limitations of the UNIFAC model.

Although the standard deviations of the measurements of malonic acid and glycerol are relatively large compared with those of the other species, they are still within the range of experimental error. The larger standard deviations for malonic acid and glycerol are attributed to errors in the stepwise measurements and higher volatility, respectively. These measurements demonstrate that the SEDB can be used to study semivolatile water-soluble organic compounds. We have attempted to measure the water activities of 1,6-hexanediol, which has a vapor pressure of 9.9×10^{-4} mmHg (ref 38). However, its fast evaporation prohibits hygroscopic measurements. The limit of the vapor pressure of a species that can be studied with the SEDB has been found to be approximately 1×10^{-4} mmHg.

Figure 2b shows that the mfs measurements for $MgSO_4$ deviate significantly from the published data. The hygroscopic growth measurements for $MgSO_4$ in the form of mfs as a function of a_w are shown in Figure 5. They deviate from the SEDB measurements of evaporating $MgSO_4$ droplets made by Ha and Chan[23] at low a_w. By comparing the time series data on $Na_2SO_4/MgSO_4$ particles with the measurements of other mixtures studied, Chan et al.[24] concluded that there is a significant mass-transfer limitation in the evaporation of $Na_2SO_4/MgSO_4$ droplets that is not found in most systems that they studied. They also observed that the evaporation rate of $MgSO_4$ droplets is about 40% less than that of $MgCl_2$ droplets of similar size and further proposed that this is because of the formation of a gel structure in $MgSO_4$ at high concentrations. Zhang and Chan[36,43] compared the Raman spectra of levitated aqueous $MgSO_4$ and $(NH_4)_2SO_4$ droplets at RH = 8.3−88.3%. They found that the spectral characteristics (the peak location and its full width at half-maximum) of the sulfate peak at ~980 cm^{-1} of $MgSO_4$ droplets change significantly at high concentrations. Such changes were not found in $(NH_4)_2SO_4$ solutions even at supersaturated conditions. They concluded that such distortion of the sulfate peak is a result of direct ion pair formation of Mg^{2+} and SO_4^{2-} ions without solvation water at water-to-solute ratios smaller than six, the number of hydration of Mg^{2+}. Zhang and Chan[36] further proposed a "polymeric" chain structure consisting of direct contact pairs at a water-to-solute molar ratio of 2.

The initial state of the particle at RH = 10% in Figure 5 was achieved by evaporation. On the basis of the above referenced work, the existence of a "polymeric" chain structure would retard the rate of both evaporation and growth at a high $MgSO_4$ concentration. Results from the SEDB growth experiments suggest that the "dried" particle (at 10% RH) starts to absorb water only at RH = 40%. From RH = 40−46%, the mfs of the $MgSO_4$ particle decreases abruptly from about 0.63 to 0.46. As a_w further increases and the droplet becomes more diluted, the measurements then follow the data obtained by Ha and Chan.[23]

Figure 6 shows the relative difference between the fractional change of voltage $((V_o - V)/(V_o - V_f))$ of $MgSO_4$, $CaCl_2$, and

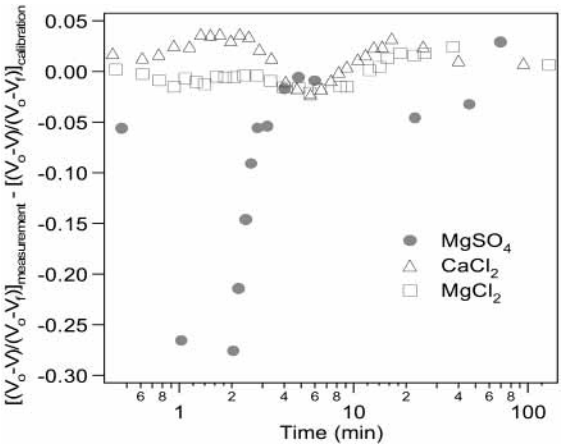

Figure 6. Relative difference of the fractional change of voltage $((V_o - V)/(V_o - V_f))$ of $MgSO_4$, $CaCl_2$, and $MgCl_2$ from the fractional change of voltage $((V_o - V)/(V_o - V_f))$ of their respective calibration curves as a function of time. V_o is the initial balance DC voltage at time zero, V is the balance voltage at time t, and V_f is the final balance voltage at the end of the experiment (after about an hour) in the SEDB measurements.

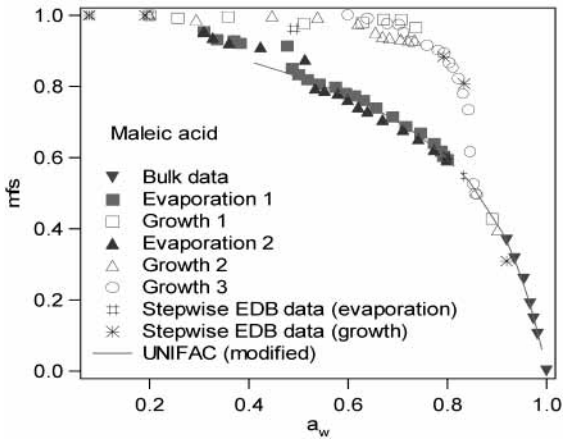

Figure 7. Water activities of maleic acid. UNIFAC (modified) represents the prediction by the modified UNIFAC equation.

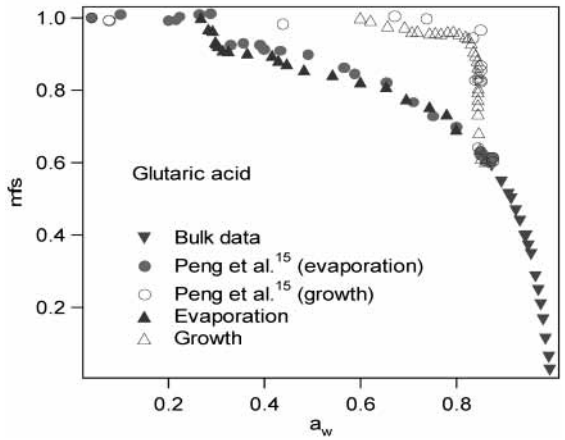

Figure 8. Water activities of glutaric acid.

$MgCl_2$ and that of their respective calibration curves based on NaBr as a function of time. All curves should have values close to zero because they should have the same transient changes as the calibration curve regardless of the nature of the solute and the size of the particles if the assumption of the quasi-equilibrium of the SEDB measurement, that is, the change of RH inside the EDB is the rate-limiting step, is valid. Figure 6 shows that the trends of the species studied are consistent with the calibrations but that of $MgSO_4$ exhibits much slower growth in the first 1.5 min of the experiment, as indicated by the negative value of the relative difference in the fractional change of the voltage between $MgSO_4$ and the calibration curve. The growth rate of $MgSO_4$ particles is only about 5% of that of other species in the first 1.5 min. This suggests that a new rate-determining step, probably the diffusion of water through a complex structural network in the droplet, is formed. An abrupt increase in the relative difference of the fractional change of voltage between $MgSO_4$ and the calibration curve appears at $t = 2$ min, which indicates that there is a sudden increase in the growth rate of $MgSO_4$. This can be explained by the "dissolution" of the network at low concentrations of $MgSO_4$. The particle then grows following the normal trend and is consistent with the calibration. The result suggests that significant mass transfer exists for both evaporation and growth of $MgSO_4$ aerosols at low RH. The above results suggest that when the mass transfer effect is significant to such an extent that it becomes a new rate-limiting step for growth or evaporation of the levitated particles in the EDB, equilibrium measurements cannot be made using the SEDB.

2. Evaporation and Growth of Organic Aerosols. In this section, the water activity measurements of aqueous droplets of maleic acid, glutaric acid, a mixture of maleic acid and malic acid, and a mixture of malonic acid and glutaric acid will be presented. The mixture data are compared with predictions from the ZSR equation and the UNIFAC model.

Figure 7 shows the water activity data of maleic acid. No literature data is available for this organic acid. Its vapor pressure is 3.6×10^{-5} mmHg (ref 38), about one-fifth of that of glycerol, which means that evaporation is therefore not a problem in our SEDB measurements. The saturation point of maleic acid is at RH = 93.1% (ref 16). Because there is no overlap between the bulk data and the reference state of the SEDB measurements, an estimation of the bulk water activities is needed. Hence, the UNIFAC model is used to calculate the mfs of this organic acid at the reference state of RH = 80%. Although maleic acid was not studied by Peng et al.,[15] the modified interaction UNIFAC parameters work well in predicting its water activity, even at high concentrations, as shown in Figure 7. Maleic acid crystallizes at RH = 48−51%, and it contains a small amount of water (8% by mass) after crystallization, which may be due to the presence of water within the crystal lattice.[44] It becomes completely anhydrous at RH < 40%. In increasing RH, maleic acid starts to absorb water at about RH = 71% and continues to deliquesce between RH = 71% and 86%. Although deliquescence usually involves an abrupt decrease in the mfs as the RH reaches a particular value, Peng et al.[15] observed the "gradual deliquescence" of oxalic acid using stepwise measurements in an EDB. We have made a few stepwise measurements, allowing about 1.5−2 h for equilibrium in each measurement. As shown in Figure 7, the stepwise measurements are close to the SEDB measurements, confirming the observation of "gradual deliquescence" after RH = 71%. The measured DRH of 71% is close to the value of 73% quoted by Clegg et al.[16]

Figure 8 shows the evaporation and growth data of glutaric acid. Peng et al.[15] measured the DRH of glutaric acid to be 83%. According to Figure 8, glutaric acid starts to absorb water at about RH = 83%, and the process is completed at RH = 85.2%. The difference between the DRH measured in our study (85.2%) and that in Peng et al.[15] (83%) is due to the mass-transfer limitation in the growth of glutaric acid, which has also been observed in the growth of sodium pyruvate[14] and $MgSO_4$.

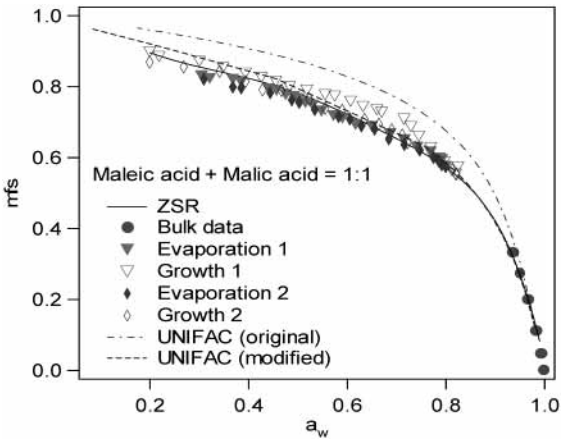

Figure 9. Water activities of equal molar mixture of maleic acid and malic acid. ZSR represents the prediction by the ZSR equation. UNIFAC (original) and UNIFAC (modified) represent the prediction by the original UNIFAC equation and the modified UNIFAC equation, respectively.

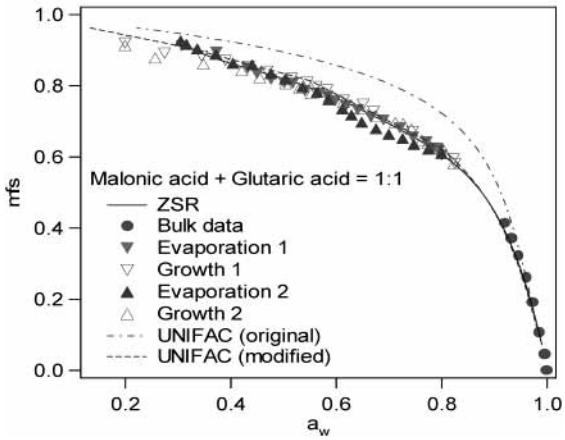

Figure 10. Water activities of equal molar mixture of malonic acid and glutaric acid. ZSR represents the prediction by the ZSR equation. UNIFAC (original) and UNIFAC (modified) represent the UNIFAC predictions using the original and the modified interaction parameters, respectively.

It should be noted that the RH_2 of this growth experiment was set at 95% because of the anticipated high DRH of glutaric acid. The time required for the RH to change from 83% to 85% (or for complete deliquescence) is 1.7 h, which is much longer than the time required in other growth experiments.

Figure 9 shows the evaporation and growth data of an equal molar mixture of maleic acid and malic acid. Malic acid is nondeliquescent in single-particle studies, and it contains about 5% water at RH < 5% (ref 15). Because the ZSR predictions are consistent with the bulk data, the ZSR equation was used to calculate the reference state. Neither crystallization nor deliquescence was observed in this mixture, and about 10% of residual water was found at RH = 20%. Suppression of the crystallization of maleic acid by the presence of noncrystallizing malic acid was clearly observed. The original UNIFAC predictions generally over estimate the a_w of the mixture but the modified UNIFAC and the ZSR predictions are in excellent agreement with the measurements. In fact, the modified UNIFAC and the ZSR predictions are so close that they are not distinguishable at low concentrations.

Figure 10 shows the evaporation and growth data of an equal molar mixture of malonic acid and glutaric acid. No mass-transfer problem was observed in the evaporation and growth of this mixture because it does not experience crystallization and deliquescence, which are the slow processes observed for glutaric acid. Malonic acid has a similar effect as malic acid on the crystallization behavior of maleic acid, suppressing the crystallization of glutaric acid. Both the ZSR and the modified UNIFAC predictions are consistent with experimental measurements.

Conclusions

We have shown that the SEDB is capable of measuring the water activities of droplets of semivolatile species with total vapor pressure below 1×10^{-4} mmHg. It is expected that this technique will be very useful in providing further valuable data on WSOC, especially on semivolatile WSOC and their mixtures. It also facilitates the observation of the transient effects in crystallization or deliquescence by providing high-resolution data in a relatively short time. However, when the change of RH inside the EDB is no longer the rate-limiting step in the evaporation or growth of droplets, such as when mass-transfer effects inside the droplets become rate-limiting, the SEDB cannot yield equilibrium measurements. Although the systems that we tested are limited, the good agreement with the modified UNIFAC predictions provides further evidence that they are suitable for predicting the water activities of mixed WSOC. Predictions of other thermodynamic properties of WSOC using the modified interaction parameters need to be tested.

Acknowledgment. This work is supported by the Research Grants Council of the Hong Kong Special Administrative Region, China (Project No. HKUST6121/97P and HKUST6039/00P).

References and Notes

(1) Intergovernmental Panel on Climate Change. *Climate change*; Cambridge University Press: New York, 1995.
(2) Charlson, R. J.; Anderson, T. L.; Rodhe, H. *Contrib. Atmos. Phys.* **1999**, *72* (1), 79.
(3) Seinfeld, J. H. *Science* **1989**, *243*, 745.
(4) Kulmala, M.; Korhonen, P.; Vesala, T.; Hansson, H.-C.; Noone, K.; Svenningsson, B. *Tellus, Ser. B* **1996**, *48*, 347.
(5) Malm, W. C.; Day, D. E. *Atmos. Environ.* **2001**, *35* (16), 2845.
(6) Ge, Z.; Wexler, A. S.; Johnston, M. V. *J. Colloid Interface Sci.* **1996**, *183*, 68.
(7) Ge, Z.; Wexler, A. S.; Johnston, M. V. *J. Phys. Chem. A* **1998**, *102*, 173.
(8) Martin, S. T. *Chem. Rev.* **2000**, *100*, 3403.
(9) Saxena, P.; Hildemann, L. M.; McMurry, P. H.; Seinfeld, J. H. *J. Geophys. Res.* **1995**, *100* (D9), 18755.
(10) Eichel, C.; Kramer, M.; Schut, L.; Wurzler, S. *J. Geophys. Res.* **1996**, *101* (D23), 29499.
(11) Malm, W. C. *Atmos. Environ.* **1997**, *31*, 1965.
(12) Cruz, C. N.; Pandis, S. N. *J. Geophys. Res.* **1998**, *103* (D11), 13111.
(13) Lightstone, J. M.; Onasch, T. B.; Imre, D.; Oatis, S. *J. Phys. Chem. A* **2000**, *104*, 9337−9346.
(14) Peng, C.; Chan, C. K. *Atmos. Environ.* **2000**, *35*, 1183.
(15) Peng, C.; Chan, M. N.; Chan, C. K. *Environ. Sci. Technol.* **2001**, *35*, 4495.
(16) Clegg, S. L.; Seinfeld, J. H.; Brimblecombe, P. *J. Aerosol Sci.* **2001**, *32*, 713.
(17) Ninni, L.; Camargo, M. S.; Meirelles, A. J. A. *J. Chem. Eng. Data* **2000**, *45*, 654.
(18) Ansari, A. S.; Pandis, S. N. *Environ. Sci. Technol.* **2000**, *34*, 71.
(19) Cohen, M. D.; Flagan, R. C.; Seinfeld, J. H. *J. Phys. Chem.* **1987**, *91*, 4563.
(20) Tang, I. N.; Munkelwitz, H. R. *J. Geophys. Res.* **1994**, *99*, 18801.
(21) Na, H. S.; Arnold, S.; Myerson, A. S. *J. Cryst. Growth* **1995**, *149*, 229.
(22) Liang, Z.; Chan, C. K. *Aerosol Sci. Technol.* **1997**, *26*, 255.
(23) Ha, Z.; Chan, C. K. *Aerosol Sci. Technol.* **1999**, *31*, 154.

(24) Chan, C. K.; Ha, Z.; Choi, M. Y. *Atmos. Environ.* **2000**, *34*, 4795.
(25) Ha, Z.; Choy, L.; Chan, C. K. *J. Geophys. Res.* **2000**, *105* (D9), 11699.
(26) Khwaja, H. A. *Atmos. Environ.* **1995**, *29* (1), 127.
(27) Kawamura, K.; Kasukabe, H. *Atmos. Environ.* **1996**, *30*, 1709.
(28) Kawamura, K.; Sempere, R.; Imai, Y.; Fujii, Y.; Hayashi, M. *J. Geophys. Res.* **1996**, *101* (D13), 18721.
(29) Saxena, P.; Hildemann, L. M. *J. Atmos. Chem.* **1996**, *24*, 57.
(30) Zdanovskii, A. B. *Zh. Fiz. Khim.* **1948**, *22*, 1475.
(31) Stokes, R. H.; Robinson, R. A. *J. Phys. Chem.* **1966**, *70*, 2126.
(32) Davis, E. J. *Aerosol Sci. Technol.* **1997**, *26*, 212.
(33) Lobo, V. M. M. *Handbook of electrolyte solutions*; Elsevier Science: New York, 1989.
(34) Perry, G. *Perry's chemical engineer's handbook*, 7th ed.; R. R. Donnelley & Sons Company: New York, 1997.
(35) Tang, I. N. *J. Geophys. Res.* **1997**, *102*, 1883.
(36) Zhang, Y. H.; Chan, C. K. *J. Phys. Chem. A* **2000**, *104*, 9191.
(37) Stokes, R. H.; Robinson, R. A. *J. Am. Chem. Soc.* **1948**, *70*, 1870.
(38) Saxena, P.; Hildemann, L. M. *Environ. Sci. Technol.* **1997**, *31*, 3318.
(39) *Ullmann's encyclopedia of industrial chemistry*, 5th ed.; VCH: Weinheim, Federal Republic of Germany, 1985.
(40) Ray, A. K.; Johnson, R. D.; Souyri, A. *Langmuir* **1989**, *5*, 133.
(41) Reid, R. C.; Prausnitz, J. M.; Poling, B. E. *The Properties of Gases and Liquids*, 4th ed.; McGraw-Hill: New York, 1987; pp 324−330.
(42) Peng, C.; Chow, A. H. L.; Chan, C. K. *Aerosol Sci. Technol.* **2001**, *35*, 753.
(43) Zhang, Y. H.; Chan, C. K. *J. Phys. Chem. A* **2002**, *106*, 285.
(44) Weis, D. D.; Ewing, G. E. *J. Geophys. Res.* **1999**, *104* (D17), 21275.